

Time-domain analysis of enhanced transmission through a single subwavelength aperture

Amit Agrawal, Hua Cao, and Ajay Nahata

Department of Electrical and Computer Engineering, University of Utah, Salt Lake City, UT 84112
nahata@ece.utah.edu

Abstract: We have measured the enhanced transmission properties of a single subwavelength aperture surrounded by periodically spaced annular grooves using time-domain techniques. While the present measurements utilize terahertz time-domain approaches, with appropriately scaled device parameters, the general observations should be applicable to other spectral ranges. In contrast to measurements that rely on continuous wave excitation and frequency domain measurements, we are able to determine the contribution of each individual groove to the transmitted terahertz waveform. Using structures containing only a single annular groove surrounding the aperture, we find that each groove can couple a large fraction of the incident terahertz bandwidth in the form of a surface wave pulse. When multiple annular grooves surround the aperture, we observe oscillations in the time-domain waveform that are temporally delayed from the initial bipolar waveform in direct relation to the distance of the groove from the aperture. This is further demonstrated by using structures containing defects (absence of annular grooves).

©2005 Optical Society of America

OCIS codes: (240.6690) Surface waves; (050.1220) Apertures

References and links

1. H. Bethe, "Theory of diffraction by small holes," *Phys. Rev.* **66**, 163-182 (1944).
2. C.J. Bouwkamp, "Diffraction theory," *Rep. Prog. Phys.* **17**, 35-100 (1954).
3. D.E. Grupp, H.J. Lezec, T. Thio, T.W. Ebbesen, "Beyond the Bethe limit: tunable enhanced light transmission through a single sub-wavelength aperture," *Adv. Mater.* **11**, 860-862 (1999).
4. T.W. Ebbesen, H.J. Lezec, H.F. Ghaemi, T. Thio, P.A. Wolff, "Extraordinary optical transmission through sub-wavelength hole arrays," *Nature* **391**, 667-669 (1998).
5. T. Thio, K.M. Pellerin, R.A. Linke, H.J. Lezec, T.W. Ebbesen, "Enhanced light transmission through a single subwavelength aperture," *Opt. Lett.* **26**, 1972-1974 (2001).
6. H.J. Lezec, A. Degiron, E. Devaux, R.A. Linke, F. Martin-Moreno, L.J. Garcia-Vidal, and T.W. Ebbesen, "Beaming light from a subwavelength aperture," *Science* **297**, 220-222 (2002).
7. T. Thio, H.J. Lezec, T.W. Ebbesen, K.M. Pellerin, G.D. Lewen, A. Nahata, R.A. Linke, "Giant optical transmission of sub-wavelength apertures: physics and applications," *Nanotechnology* **13**, 429-432 (2002).
8. A. Nahata, R.A. Linke, T. Ishi, and K. Ohashi, "Enhanced nonlinear optical conversion using periodically nanostructured metal films," *Opt. Lett.* **28**, 423-425 (2003).
9. M.J. Lockyear, A.P. Hibbins, J.R. Sambles, C.R. Lawrence, "Surface-topography-induced enhanced transmission and directivity of microwave radiation through a subwavelength circular metal aperture," *Appl. Phys. Lett.* **84**, 2040-2042 (2004).
10. A. Degiron and T. W. Ebbesen, "Analysis of the transmission process through single apertures surrounded by periodic corrugations," *Opt. Express* **12**, 3694-3700 (2004), <http://www.opticsexpress.org/abstract.cfm?URI=OPEX-12-16-3694>.
11. H. J. Lezec and T. Thio, "Diffracted evanescent wave model for enhanced and suppressed optical transmission through subwavelength hole arrays," *Opt. Express* **12**, 3629-3651 (2004), <http://www.opticsexpress.org/abstract.cfm?URI=OPEX-12-16-3629>.
12. A.P. Hibbins, J.R. Sambles, and C.R. Lawrence, "Gratingless enhanced microwave transmission through a subwavelength aperture in a thick metal plate," *Appl. Phys. Lett.* **81**, 4661-4663 (2002).
13. M.J. Lockyear, A.P. Hibbins, J.R. Sambles, and C.R. Lawrence, "Enhanced microwave transmission through a single subwavelength aperture surrounded by concentric grooves," *J. Opt. A: Pure Appl. Opt.* **7**, S152-S158 (2005).
14. S.S. Akarca-Biyikli, I. Bulu, and E. Ozbay, "Enhanced transmission of microwave radiation in one-dimensional metallic gratings with subwavelength aperture," *Appl. Phys. Lett.* **85**, 1098-2000 (2004).

15. H. Cao, A. Agrawal, and A. Nahata, "Controlling the transmission resonance lineshape of a single subwavelength aperture," *Opt. Express* **13**, 763-769 (2005), <http://www.opticsexpress.org/abstract.cfm?URI=OPEX-13-3-763>.
16. F. J. Garcia-Vidal, L. Martin-Moreno, H. J. Lezec and T. W. Ebbesen, "Focusing light with a single subwavelength aperture flanked by surface corrugations," *Appl. Phys. Lett.* **83**, 2000-2002 (2003).
17. L. Martin-Moreno, F.J. Garcia-Vidal, H. J. Lezec, A. Degiron, and T.W. Ebbesen, "Theory of highly directional emission from a single subwavelength aperture surrounded by surface corrugations," *Phys. Rev. Lett.* **90**, 167401/1-4 (2003).
18. M.M.J. Treacy, "Dynamical diffraction in metallic optical gratings," *Appl. Phys. Lett.* **75**, 606-608 (1999).
19. Q. Cao and P. Lalanne, "Negative role of surface plasmons in the transmission of metallic gratings with very narrow slits," *Phys. Rev. Lett.* **88**, 057403/1-4 (2002).
20. D. Grischkowsky, in *Frontiers in Nonlinear Optics*, edited by H. Walther, N. Koroteev, and M.O. Scully (Institute of Physics Publishing, Philadelphia, 1992) and references therein.
21. H. Cao and A. Nahata, "Influence of aperture shape on the transmission properties of a periodic array of subwavelength apertures," *Opt. Express* **12**, 3664-3672 (2004), <http://www.opticsexpress.org/abstract.cfm?URI=OPEX-12-16-3664>.
22. J. Gomez Rivas, M. Kuttge, P. Haring Bolivar, H. Kurz, and J.A. Sanchez-Gil, "Propagation of surface plasmon polaritons on semiconductor gratings," *Phys. Rev. Lett.* **93**, 256804/1-4 (2004).

1. Introduction

A broad range of near-field electromagnetic techniques and applications rely on the use of a single subwavelength aperture to restrict the spatial properties of the transmitted electromagnetic radiation. While a reduction of the aperture diameter in the subwavelength regime may be used to increase the achievable spatial resolution, there is a corresponding power law decrease in the transmitted electromagnetic power [1,2]. Grupp et al. showed that by surrounding a single aperture with periodically spaced surface corrugations, the optical transmission could be strongly enhanced at wavelengths corresponding to the period spacing [3]. This finding was analogous to the initial demonstration in this area of enhanced optical transmission through a periodic array of subwavelength apertures [4]. Based on these initial demonstrations, there has been significant work in trying to understand the underlying physical mechanisms behind the phenomenon. Such an understanding should allow for the development of unique and useful technologies based on this effect.

To date, there have been a number of experimental [3, 5-15] and theoretical [16-19] investigations into the transmission properties of single subwavelength aperture surrounded by periodic surface corrugations. The most common embodiment of this structure is the bullseye design, which is comprised of a single aperture surrounded by periodically spaced concentric annular grooves [5-11, 13, 15]. One issue that is important for understanding this phenomenon regards the role that the periodic scattering sites, concentric annular grooves in our case, play in the transmission enhancement process. There have been several studies that have explored the role of the scattering sites by employing bullseye patterns with varying numbers of annular grooves. When only one annular groove surrounds the subwavelength aperture, it has been shown that the transmission at the resonant wavelength is enhanced, though only modestly. Based on this observation, Hibbins et al. discuss the enhanced transmission effect in terms of the coupling together of cavity modes in the grooves [12]. Lezec and Thio, on the other hand, describe their observations in terms of composite diffractive evanescent waves [11]. It should be noted that the corresponding experimental studies utilized only frequency domain characterization techniques.

In this submission, we measure the time-domain transmission properties of bullseye structures using conventional terahertz (THz) time-domain spectroscopy. The approach allows us to uniquely determine the contribution of each annular groove to the transmitted THz time-domain waveform. Using structures containing only a single annular groove, we find that each groove can efficiently couple a large fraction of the incident THz bandwidth to surface wave modes. At metal dielectric interfaces, these surface waves are in the form of surface plasmon-polaritons. When multiple annular grooves surround the aperture, the transmitted THz waveform consists of a superposition of oscillations arising from the coupling of the incident THz pulse to a surface wave pulse by each annular groove. These oscillations are temporally

shifted from one another in accordance with the spatial distance between the grooves. We further demonstrate this by using bullseye structures containing defects (absence of annular grooves). When the phase conditions between these oscillations are set appropriately, the transmitted THz power at the resonant wavelength is enhanced relative to an equivalent bare aperture. It is worth noting that while the time-integrated THz power through the bullseye structure is greater than that through an equivalent bare aperture, at no point in time is the instantaneous electric field transmitted through the bullseye structure greater than the maximum instantaneous electric field transmitted through the bare aperture.

2. Experimental details

We fabricated and analyzed a broad range of bullseye patterns to measure the time-domain properties of the transmitted THz electric field. All of the structures were produced by chemical etching on freestanding 150 μm thick stainless steel foils. Each bullseye structure consisted of a single 490 μm diameter circular aperture surrounded by a variable number of concentric annular grooves. The typical groove width and depth was 500 μm and 100 μm , respectively and have rectangular cross-section. The typical center-to-center groove spacing was 1 mm, unless noted otherwise below. Three different sets of bullseye structures were fabricated for these studies. In the first set of samples, we fabricated only one annular groove, at consecutive groove positions, around each single subwavelength aperture. In the second set of samples, we varied the number of annular grooves surrounding the aperture. Finally, in the third set of samples, we fabricated bullseye patterns that nominally contained 10 annular grooves. In these samples, we intentionally removed specific grooves (defects). For reference purposes, we fabricated 490 μm diameter bare apertures in the same metal foils.

We used a conventional time-domain THz spectroscopy setup [20] to characterize the bullseye structures and bare apertures. Using this method, the time-domain properties of a single cycle electromagnetic transient transmitted through a structure can be measured using coherent detection with subpicosecond temporal resolution. Photoconductive devices were used for both emission and coherent detection. An off-axis paraboloidal mirror was used to collect and collimate the THz radiation from the emitter to the samples. The THz beam was normally incident on the corrugated surface of the bullseye structures. In all experiments, the THz beam, with a 1/e beam diameter of approximately 20 mm was incident on the corrugated surface at normal incidence. It is important to note that the frequency content of the THz beam varies spatially, thus the temporal properties of the incident THz pulse are also spatially dependent. The nominal frequency content of the incident beam extends from ~ 0.05 THz ($\lambda = 6000$ μm) to ~ 1 THz ($\lambda = 300$ μm), with a center frequency of ~ 0.4 THz ($\lambda = 750$ μm).

3. Experimental results and discussion

Photographs and schematic cross-sectional views of single annular groove bullseye structures are shown in Figs. 1(a) and 1(b), respectively. The radius of the center of the annular groove for the 4 upper structures, shown in Fig. 1(b), vary as $R_K = KP$, where $K = 3, 4, 5, 6$ and $P = 0.8$ mm. Thus, K is simply the groove number as one counts outward from the aperture. The measured temporal waveforms corresponding to the transmitted THz pulses through these structures are shown in Fig. 1(c). As shown at the bottom of Fig. 1(c), the transmitted waveform for the reference bare aperture is characterized by a single bipolar THz waveform. With the addition of an annular groove, an oscillation that is temporally shifted from the initial bipolar pulse and of smaller magnitude is superposed on the transmitted THz waveform. Specifically, as the spacing between the annular groove and the central aperture increases linearly ($K = 3$ to $K = 6$), there is a corresponding linear increase in the time delay between the initial bipolar waveform and the oscillation contribution from the annular groove. This process is shown graphically in Fig. 2(a). It is worth noting that this observation is consistent with our earlier finding that there are two independent, yet phase-coherent, transmission processes that contribute to the transmitted time-domain waveform: a non-resonant transmission contribution related to transmission through the subwavelength aperture

and a resonant transmission contribution related to the interaction of the THz pulse with the structured metal surface [15,21]. We attribute the decrease in the magnitude of the oscillation with increasing K primarily to the spatial profile of the incident THz beam. Using the temporal data shown in Fig. 1(c), it should be possible to determine the propagation properties of the THz surface waves [22].

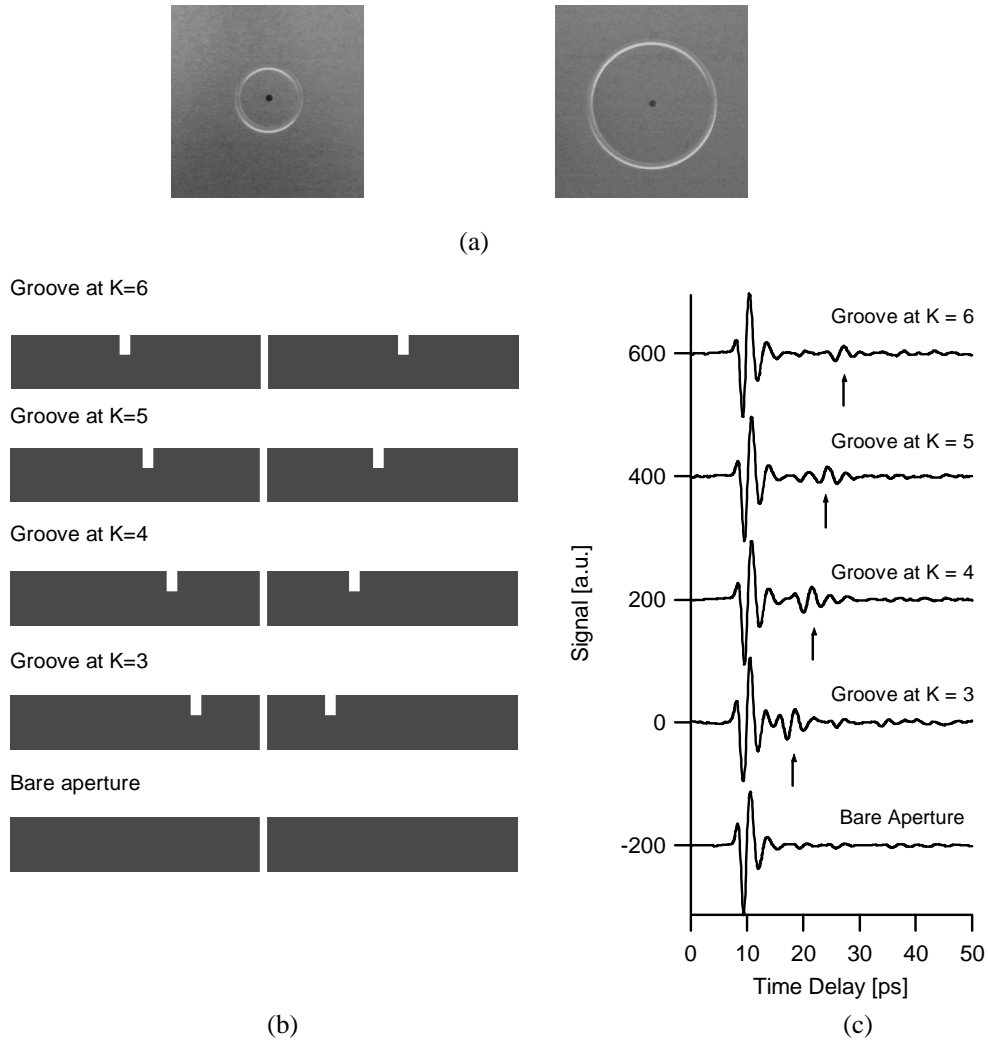


Fig. 1. (a) Photographs of typical bullseye structures consisting of only one annular groove (b) Cross-sectional line diagrams of the structures used. The radius of the center of the annular groove for the 4 upper structures shown in Fig. 1B vary at $R_K = KP$, where $K = 3, 4, 5, 6$ and $P = 0.8$ mm. (c) Five experimentally observed time-domain waveforms for the structures shown in part (b). The temporal waveforms have been offset from the origin for clarity. The arrows point to the oscillation that arises from coupling of the incident THz pulse to a surface wave pulse. The temporal change in the location of this oscillation corresponds directly to the change in distance of the annular groove from the aperture. The decrease in the magnitude of the oscillations with increasing K is related to the spatial profile of the incident THz beam.

As mentioned above, each annular groove couples a relatively large fraction of the incident THz wave to surface waves. To demonstrate this, consider bullseye structure with a single annular groove with $K=4$, for which the corresponding time-domain waveform is

shown again in Fig. 2(b). The trace consists of two components: a temporal waveform containing the initial bipolar pulse that is nominally identical to the time-domain waveform of the bare aperture and an oscillation related to the coupling properties of the annular groove, shown in the blue box in Fig. 2(b). We numerically separate these two contributions and plot the resulting amplitude spectra in Fig. 2(c). The reduced high frequency content in the time-delayed oscillation is believed to be due to the coupling properties of the annular groove. It should be noted, however, that the temporal properties of the initial bipolar pulse and any time-delayed oscillations are not expected to be identical, since the frequency content of the THz beam is spatially dependent.

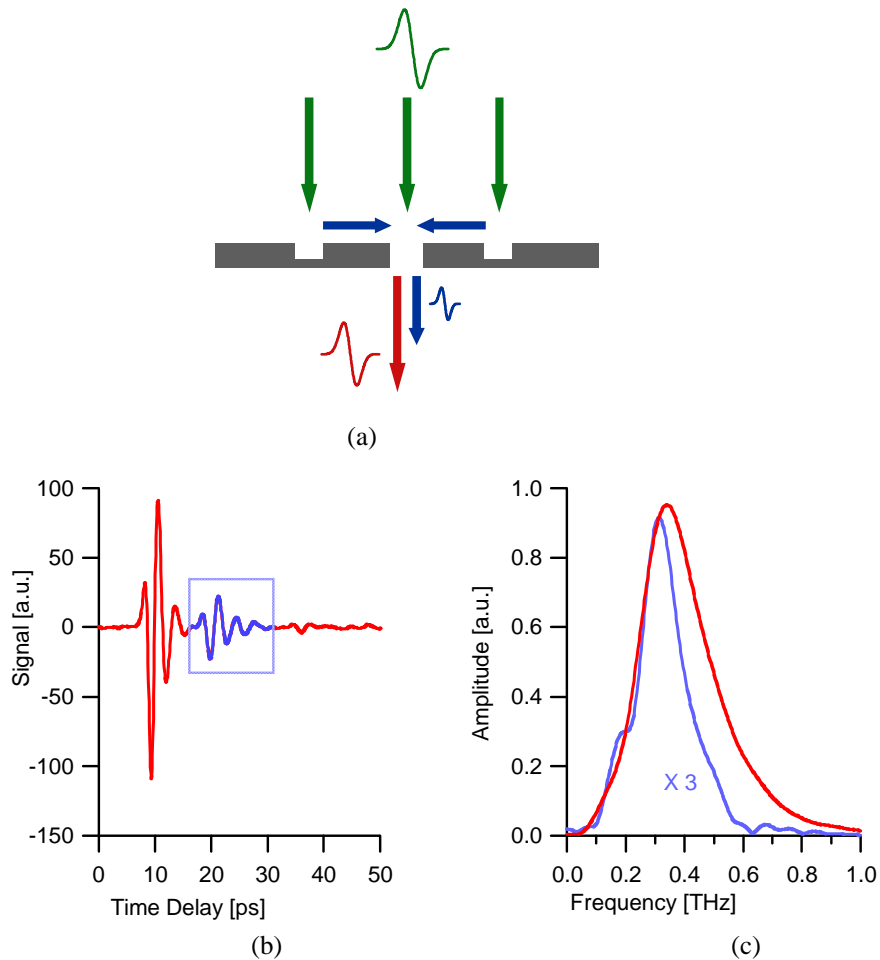


Fig. 2. (a) Schematic drawing showing the two contributions to the transmitted THz time-domain waveform. The component shown by the red arrow corresponds to the non-resonant transmission of the incident THz pulse through the subwavelength aperture. The component shown by the blue arrow corresponds to the contribution that arises from the interaction of the incident THz pulse with the structured surface. This latter component is smaller than the non-resonant component and temporally delayed. (b) Time-domain waveform for $K=4$ from Fig. 1A. The blue portion of the temporal waveform corresponds to the contribution that arises from coupling of the incident THz pulse by the annular groove (C) Amplitude spectra of the initial bipolar waveform (red) and the time-delayed oscillation (blue). The blue trace has been multiplied by a factor of 3.

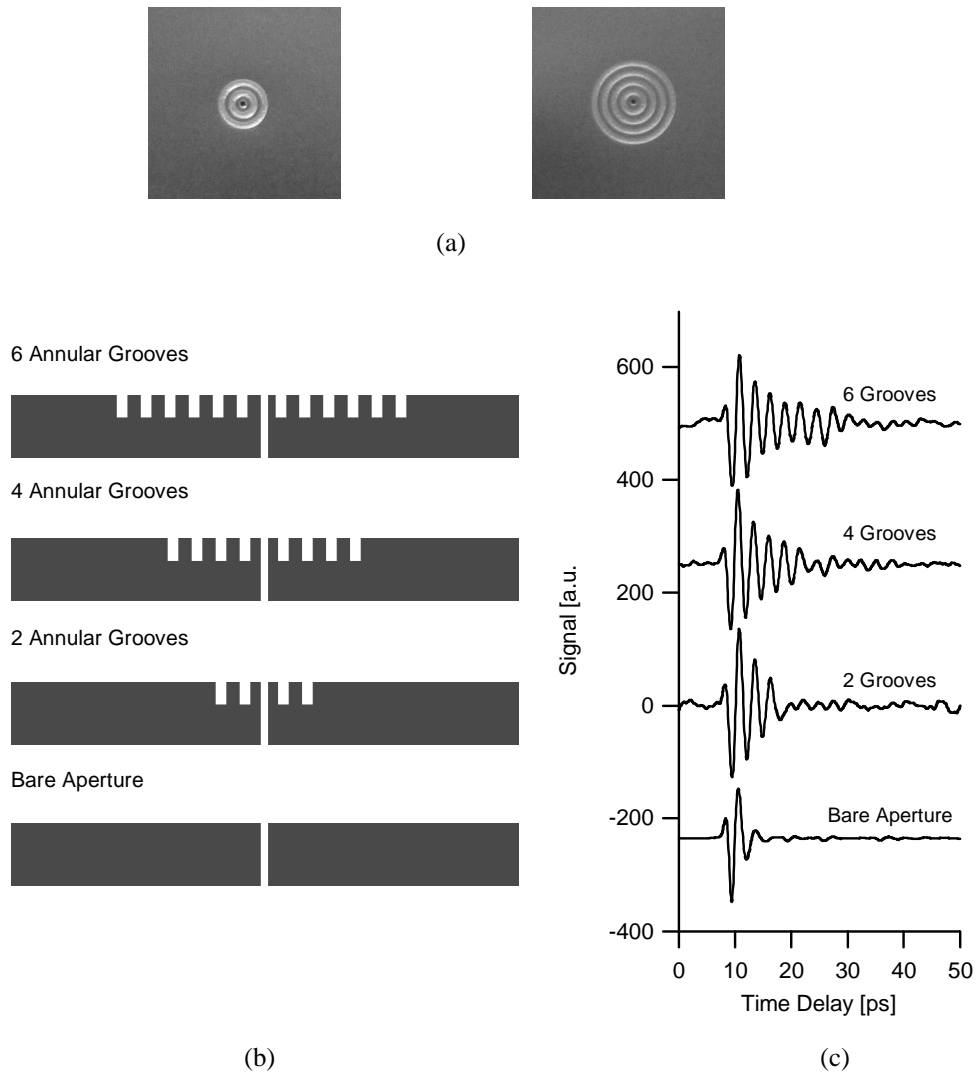


Fig. 3. (a) Photographs of typical bullseye structures consisting of periodic multiple annular grooves (b) Cross-sectional line diagrams of the structures used (c) Five experimentally observed time-domain waveforms for the structures shown in part (b). The temporal waveforms have been offset from the origin for clarity. The number of oscillations, after the initial bipolar waveform, matches the number of annular grooves.

Based on the results for single groove structures, we analyzed bullseye patterns that contained multiple annular grooves that were periodically spaced. Photographs and schematic cross-sectional views of these structures are shown in Figs. 3(a) and 3(b), respectively. The measured temporal waveforms corresponding to the transmitted THz pulses through 2, 4, and 6 groove patterns are shown in Fig. 3(c). For completeness, we also provide the transmitted waveform for the reference bare aperture. A striking aspect of the data is the one-to-one correspondence between the number of grooves and the number of oscillations after the initial bipolar pulse. As discussed above, each groove couples a fraction of the incident THz pulse to a surface wave that propagates both towards and away from the aperture. In the present geometry, only surface waves that propagate towards the aperture contribute to the transmitted THz waveform. From Fig. 3(c), it is apparent that there are a number of low amplitude oscillations following the primary oscillations. These secondary oscillations are believed to be

caused by in-plane scattering from adjacent grooves. Since the linewidth of any transmission resonance associated with these bullseye structures is much narrower than the bandwidth of the incident or coupled THz pulses, we do not expect to observe any significant formation of standing wave patterns.

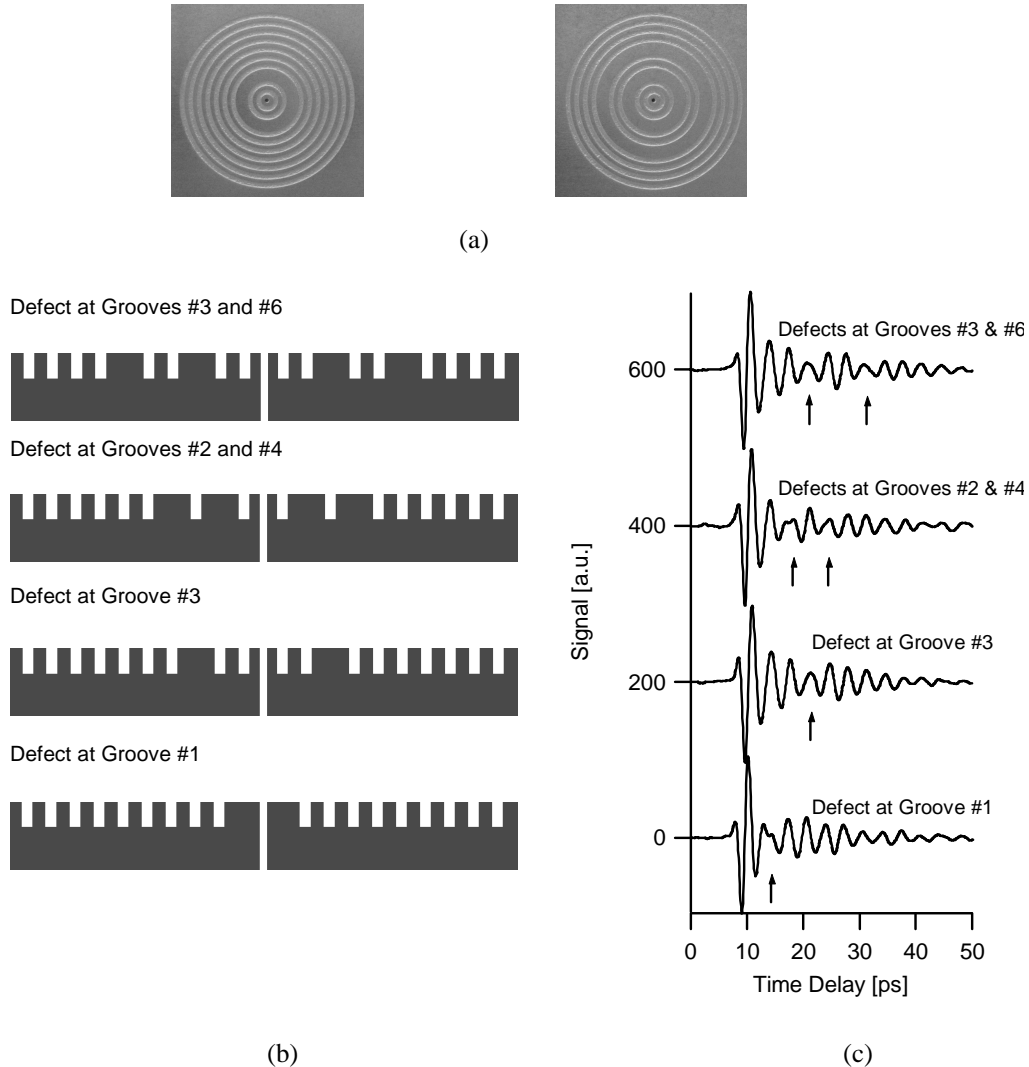


Fig. 4. (a) Photographs of typical bullseye structures containing defects (absence of annular grooves) (b) Cross-sectional line diagrams of the structures used (c) Five experimentally observed time-domain waveforms for the structures shown in part (b). The temporal waveforms have been offset from the origin for clarity. The arrows point to the temporal locations of the defects. The suppressed oscillation at the temporal location of the defect can be attributed primarily to the superposition of the trailing portion of the oscillation from the preceding groove and the leading portion of the oscillation from the following groove.

In order to obtain transmission enhancement from these bullseye structures at THz frequencies, definite phase requirements must be met. Specifically, transmission enhancement occurs when all of the constituent oscillations in the time-domain THz waveform, including the initial bipolar pulse and each coupled surface wave pulse, are equally spaced temporally. The time delay between oscillations is inversely related to the resonance frequency. By

increasing the number of grooves surrounding the aperture, the amount of radiation coupled to surface wave modes increases thereby increasing the enhancement factor. The increase in the number of oscillations following the initial pulse also corresponds to a decrease in the resonance linewidth. With bullseye structures, the phase conditions can be altered to yield transmission enhancement, transmission suppression, or a combination of the two processes at the resonant wavelength [15].

We have previously shown that by using a bullseye structure that was nominally identical to those described in Fig. 2, but containing 25 annular grooves, we were able to enhance the transmitted THz power at the resonance frequency by a factor of approximately 16 relative to an equivalent bare aperture [15]. Altering the number of grooves would lead to a commensurate change in the number of oscillations in the time-domain waveform, thereby altering the enhancement factor. In the case of the structures shown in Fig. 2, the measured enhancement factor in the transmitted THz power at the resonant frequency of 0.29 THz for the two, four, and six groove bullseye structures was 5.5, 9, and 11, respectively, when compared to an equivalent bare aperture. The relatively modest increase in the enhancement factor with an increasing number of annular grooves is attributed to the finite spatial properties of the incident THz beam.

To further investigate the role of each annular groove, we fabricated and analyzed bullseye structures that all nominally extended out to 10 annular grooves. Photographs and schematic cross-sectional views of these structures are shown in Figs. 4(a) and 4(b), respectively. The measured temporal waveforms corresponding to the transmitted THz pulses through these defect structures are shown in Fig. 4(c). In the figure, arrows point to the corresponding temporal location of the defect. Based on the discussion above, one might initially expect no oscillation whatsoever at the temporal locations of the defects. However, by looking carefully at the time-domain waveforms in Fig. 1(c) for the single annular groove structures, we find that the total temporal extent of the oscillation can be relatively long. Thus, the suppressed oscillation at the temporal location of the defect can be attributed primarily to the superposition of the trailing portion of the oscillation from the preceding groove and the leading portion of the oscillation from the following groove. For example, if we consider the structure with a defect at groove #3, the suppressed oscillation is due to the temporal overlap of the oscillations from grooves #2 and #4. The results are consistent with simulations involving the superposition of individual oscillations with varying time-delays.

4. Conclusion

In conclusion, we have measured the enhanced terahertz transmission properties of a single subwavelength aperture surrounded by surface corrugations using terahertz time-domain spectroscopy. The approach allows us to measure the individual contribution of each annular groove to the transmitted THz waveform. Using structures containing only a single annular groove surrounding the aperture, we find that each groove can couple a large fraction of the incident THz bandwidth to propagating surface waves. When multiple annular grooves surround the aperture, each annular groove couples the incident THz waveform to surface waves in the form of a time-domain oscillation. When appropriate phasing conditions exist between these contributions, the transmission is enhanced at the resonant frequency corresponding to the inverse of the time delay between oscillations. When defects (absence of annular grooves) are introduced into the surface corrugation pattern, we observe a suppressed oscillation at its corresponding temporal locations. Through optimization of groove parameters, we may be able to further suppress these oscillations at the defect locations. Thus, we would be able to control the number of oscillations and nulls (from defects), which may be important in applications requiring shaped THz pulses.